ENVIRONMENTAL DATA SCIENCE (2026), **xx**:xx 1–6

CAMBRIDGE
UNIVERSITY PRESS

APPLICATION PAPER

One Stone Three Birds: Three-Dimensional Implicit Neural Network for Compression and Continuous Representation of Multi-Altitude Climate Data

Alif Bin Abdul Qayyum[1], Xihaier Luo[3], Nathan M. Urban[3], Xiaoning Qian[1,2,3] and Byung-Jun Yoon[1,3]

[1]Department of Electrical and Computer Engineering, Texas A&M University, College Station, 77843-3128, TX, USA.
E-mail: {alifbinabdulqayyum,xqian,bjyoon}@tamu.edu.
[2]Department of Computer Science and Engineering, Texas A&M University, College Station, 77843-3112, TX, USA.
[3]Computing and Data Sciences, Brookhaven National Laboratory, Upton, 11973-5000, NY, USA.
E-mail: {xluo,nurban,xqian1,byoon}@bnl.gov.

A. Supplementary Materials

A.1. Evaluation Metrics

A.1.1. Peak Signal to Noise Ratio(PSNR)

PSNR measures the ratio between the peak signal power and noise power present in the signal. For a super resolved predicted output $\hat{\mathbf{x}}$, and its corresponding ground-truth $\mathbf{x}$, the peak signal to noise ratio is calculated using the following formula:

$$\mathbf{PSNR}(\mathbf{x}, \hat{\mathbf{x}}) = 10 \log_{10} \left(\frac{(\mathrm{MAX}(\mathbf{x}) - \mathrm{MIN}(\mathbf{x}))^2}{\frac{1}{s^2 hw} \sum_{x^c} (\mathbf{x}(x^{(c)}) - \hat{\mathbf{x}}(x^{(c)}))^2} \right)$$

A.1.2. Structural Similarity Index Measure(SSIM)

SSIM measures the similarity between two images. SSIM is widely used metric for evaluation of super resolution of images or uniform 2D grid like data. For a super resolved predicted output $\hat{\mathbf{x}}$, and its corresponding ground-truth $\mathbf{x}$, the structural similarity index measure between the window w_x of $\mathbf{x}$ and window $w_{\hat{x}}$ is calculated using the following formula:

$$\mathbf{SSIM}(\mathbf{x}_{w_x}, \hat{\mathbf{x}}_{w_{\hat{x}}}) = \frac{(2\mu_x \mu_{\hat{x}} + c_1)(2\sigma_{x\hat{x}} + c_2)}{(\mu_x^2 + \mu_{\hat{x}}^2 + c_1)(\sigma_x^2 + \sigma_{\hat{x}}^2 + c_2)}$$

Here,

- μ_x =Sample mean of window w_x
- $\mu_{\hat{x}}$ =Sample mean of window $w_{\hat{x}}$
- σ_x^2 =Variance of window w_x
- $\sigma_{\hat{x}^2}$ =Variance of window $w_{\hat{x}}$
- $\sigma_{x\hat{x}}$ =Covariance of windows w_x and $w_{\hat{x}}$
- $c_1 = (k_1 L)^2, c_2 = (k_2 L)^2$
- $k_1 = 0.01, k_2 = 0.03$
- L is the range of values for $\mathbf{x}$ and $\hat{x}$, $L = 2$ is chosen as the range is $[-1, 1]$

A.1.3. Learned Perceptual Image Patch Similarity(LPIPS)

LPIPS is a perceptual similarity metric that leverages the feature representations learned by a pre-trained deep convolutional neural network (CNN), such as AlexNet (Krizhevsky et al 2012), VGG (Simonyan and Zisserman 2014), SqueezeNet (Hu et al 2018) or a fine-tuned version of them. In this work, we utilize the SqueezeNet (Hu et al 2018) model for evaluating this metric.

LPIPS operates by comparing the feature activations of two images: a reference image, I, and a test image, $\hat{I}$, rather than their raw pixel values. The mathematical formulation for the LPIPS metric between two images I and $\hat{I}$ is given by:

$$\mathbf{LPIPS}(I, \hat{I}) = \sum_{i=1}^{L} w_i \|\phi_i(I) - \phi_i(\hat{I})\|_2^2 \tag{A.1}$$

Here, ϕ_i's are the pretrained model weights and w_i's are layer specific weights.

A.1.4. Compression Ratio(CR)

Compression ratio is the widely used metric for evaluation of data compression. For the compressed data representation $\mathbf{x}_{comp}$, and its corresponding uncompressed data representation $\mathbf{x}$, the compression ration can be calculated using the following formula:

$$\mathbf{CR} = \left(1 - \frac{\text{memory size of } \mathbf{x}_{comp}}{\text{memory size of } \mathbf{x}}\right) \times 100$$

A.2. Hyperparameter Details

Table 1 shows the list of hyperparameters utilized in this work.

Table 1. *List of hyperparamters.*

OSTB (One Stone Three Bird)	
Residual Implicit Neural Block	4

Residual Implicit Neural Block					
GAAM		Positional Encoder		MLP	
Feature	64	σ	25	Hidden Dimension	256
Head	1	m	30	Layer	2
-	-	-	-	Output Dimension	64

Implicit Super Resolution Decoder			
EDSR Feature Encoder		KAN Decoder	
Feature	64	Hidden Layer	2
Residual Block	4	Neuron	32
Residual Scale	1	Grid Size	5
-	-	Spline Order	3
-	-	Scale Noise	0.1
-	-	Base Scale	1
-	-	Spline Scale	1
-	-	Grid Epsilon	0.02
-	-	Grid Range	[-1, 1]

A.3. Comparative Performance across Cross-Altitude Configurations

Figure 1 shows the performance of the OSTB model at different cross-altitude prediction scenarios. For both PSNR and SSIM, the OSTB model performs better when h_{in} is $60m$, compared to the scenario when h_{in} is $10m$. Also, for a fixed h_{in}, the OSTB model performs better when h_{out} is closer to h_{in}. This observation indicates that the model's performance increases with decreasing $(h_{out} - h_{in})$. For LPIPS, the performance primarily depends on the h_{out}, and the overall performance is better for $h_{out} = 200m$, compared to $h_{out} = 160m$.

A.4. Additional Experiment: Comparison with Baselines

A.4.1. Task

We evaluated the model's continuous reconstruction capability by performing super-resolution at different scales on a test dataset containing 800 data points. As we split each data point into 4 regions, the total number of effective test data samples is 3200.

A.4.2. Setup

High-resolution input dimension was set to 120×160, with a dimension reduction factor $d = 8$, yielding a low-resolution representation of 15×20. We focus on cross-altitude predictions where the output modality height h_{in} is closer to the ground (10m, 60m) and the input modality height h_{out} is significantly higher (160m, 200m).

A.4.3. Result Summary

As shown in Figure 2, our model consistently outperforms all the baselines across all cross-altitude scenarios and super-resolution scales for PSNR and SSIM. Our model obtained low LPIPS for super resolution scale 2×, but obtained higher LPIPS for higher super resolution scales. GINO model obtained superior results in terms of LPIPS. Results for super-resolution scales $s \in [2, 4]$ and $s \in [5, 6]$ respectively illustrate the results for in-distribution scales and out-of-distribution scales.

A.5. Additional Experiment: Data Compression

We report the compression performaces for cross-altitude scenarios where the output modality h_{out} is closer to the ground (10m, 60m) and the input modality is much higher above from the ground (160m, 200m) at Table 2.

Our proposed OSTB model outperforms the other data compression baselines in most cases, except those cross-altitude prediction scenarios where $h_{out} = 60m$. Those baselines which achieve superior PSNR, SSIM and LPIPS, does this at the cost of a lower compression ratio.

A.6. Additional Experiment: Modality Transfer

We evaluate the performance of our model without the 3D ETINN segment by designing and training separate models for different altitude levels, then comparing them in cross-altitude prediction tasks in scenarios where the output modality (h_{out}) is closer to the ground and the input modality (h_{in}) is much higher above from the ground.

Figure 3 presents the average PSNR, SSIM and LPIPS across the test set at different super-resolution scales. In all cross-altitude prediction scenarios, the model incorporating the 3D ETINN consistently outperforms the models without it (except for SSIM and LPIPS at cross-altitude scenarios where $h_{out} = 60m$).

Table 2. *Comparative compression performance at different cross-altitude prediction scenarios.*

Model	h_{in} = 160m → h_{out} = 10m				h_{in} = 200m → h_{out} = 10m			
	PSNR(↑)	SSIM(↑)	LPIPS(↓)	CR(↑)	PSNR(↑)	SSIM(↑)	LPIPS(↓)	CR(↑)
PPM$_{Q=4,\alpha=0.16}$	17.3636	0.3563	0.3980	97.7531	17.6259	0.3553	0.3925	97.8359
PPM$_{Q=4,\alpha=0.24}$	19.3376	0.3619	0.3647	97.7531	19.7455	0.3618	0.3593	97.8359
PPM$_{Q=4,\alpha=0.32}$	21.2912	0.3706	0.3412	97.7531	21.8357	0.3722	0.3378	97.8359
PPM$_{Q=8,\alpha=0.16}$	27.0938	0.5699	0.2260	96.6117	26.7788	0.5545	0.2308	96.6998
PPM$_{Q=8,\alpha=0.24}$	28.6932	0.5967	0.2106	96.6117	28.4758	0.5822	0.2151	96.6998
PPM$_{Q=8,\alpha=0.32}$	29.9741	0.6147	0.2009	96.6117	29.8059	0.5997	0.2059	96.6998
PPM$_{Q=12,\alpha=0.16}$	30.3472	0.6709	0.1659	95.5304	30.1427	0.6506	0.1730	95.6702
PPM$_{Q=12,\alpha=0.24}$	31.7768	0.6961	0.1562	95.5304	31.6171	0.6758	0.1641	95.6702
PPM$_{Q=12,\alpha=0.32}$	32.6256	0.7037	0.1539	95.5304	32.4340	0.6819	0.1635	95.6702
PPM$_{Q=16,\alpha=0.16}$	31.8551	0.7178	0.1360	94.7703	31.4296	0.6916	0.1453	94.9265
PPM$_{Q=16,\alpha=0.24}$	33.0246	**0.7378**	**0.1311**	94.7703	32.6434	0.7118	**0.1413**	94.9265
PPM$_{Q=16,\alpha=0.32}$	33.4298	0.7367	0.1343	94.7703	33.0543	0.7095	0.1464	94.9265
Bicubic$_{d=4,\alpha=0.16}$	33.6326	0.7245	0.3395	93.7500	33.2154	0.7048	0.3432	93.7500
Bicubic$_{d=4,\alpha=0.24}$	34.0809	0.7360	0.3375	93.7500	33.7382	**0.7161**	0.3419	93.7500
Bicubic$_{d=4,\alpha=0.32}$	33.7710	0.7263	0.3401	93.7500	33.4583	0.7048	0.3459	93.7500
Bicubic$_{d=8,\alpha=0.16}$	32.9835	0.6808	0.5720	**98.4375**	32.6601	0.6667	0.5675	**98.4375**
Bicubic$_{d=8,\alpha=0.24}$	33.5205	0.6952	0.5462	**98.4375**	33.2654	0.6810	0.5411	**98.4375**
Bicubic$_{d=8,\alpha=0.32}$	33.3362	0.6906	0.5262	**98.4375**	33.0974	0.6746	0.5211	**98.4375**
OSTB*	**34.1774**	0.7261	0.4137	**98.4375**	**33.9153**	0.7105	0.4153	**98.4375**
Model	h_{in} = 160m → h_{out} = 60m				h_{in} = 200m → h_{out} = 60m			
	PSNR(↑)	SSIM(↑)	LPIPS(↓)	CR(↑)	PSNR(↑)	SSIM(↑)	LPIPS(↓)	CR(↑)
PPM$_{Q=4,\alpha=0.16}$	15.0797	0.3390	0.4477	97.7531	15.3487	0.3389	0.4402	97.8359
PPM$_{Q=4,\alpha=0.24}$	15.7955	0.3380	0.4300	97.7531	16.2231	0.3379	0.4196	97.8359
PPM$_{Q=4,\alpha=0.32}$	16.5111	0.3373	0.4138	97.7531	17.0965	0.3375	0.4015	97.8359
PPM$_{Q=8,\alpha=0.16}$	25.3426	0.5755	0.2494	96.6117	25.0440	0.5603	0.2545	96.6998
PPM$_{Q=8,\alpha=0.24}$	25.9676	0.5838	0.2414	96.6117	25.7960	0.5698	0.2449	96.6998
PPM$_{Q=8,\alpha=0.32}$	26.5575	0.5910	0.2342	96.6117	26.4933	0.5778	0.2367	96.6998
PPM$_{Q=12,\alpha=0.16}$	29.4231	0.7124	0.1748	95.5304	29.1651	0.6876	0.1820	95.6702
PPM$_{Q=12,\alpha=0.24}$	30.0411	0.7214	0.1693	95.5304	29.8836	0.6974	0.1757	95.6702
PPM$_{Q=12,\alpha=0.32}$	30.5884	0.7274	0.1645	95.5304	30.4934	0.7030	0.1705	95.6702
PPM$_{Q=16,\alpha=0.16}$	31.4576	0.7749	0.1355	94.7703	30.9130	0.7424	0.1452	94.9265
PPM$_{Q=16,\alpha=0.24}$	32.0158	0.7820	0.1312	94.7703	31.5583	0.7502	0.1407	94.9265
PPM$_{Q=16,\alpha=0.32}$	32.4492	**0.7853**	**0.1280**	94.7703	32.0224	0.7527	**0.1378**	94.9265
Bicubic$_{d=4,\alpha=0.16}$	34.3314	0.7763	0.3353	93.7500	33.6705	0.7527	0.3391	93.7500
Bicubic$_{d=4,\alpha=0.24}$	**34.5598**	0.7787	0.3348	93.7500	**33.9373**	**0.7551**	0.3389	93.7500
Bicubic$_{d=4,\alpha=0.32}$	34.4659	0.7769	0.3348	93.7500	33.8196	0.7517	0.3394	93.7500
Bicubic$_{d=8,\alpha=0.16}$	33.1275	0.7106	0.6081	**98.4375**	32.6761	0.6956	0.6029	**98.4375**
Bicubic$_{d=8,\alpha=0.24}$	33.3903	0.7140	0.5980	**98.4375**	32.9868	0.6992	0.5911	**98.4375**
Bicubic$_{d=8,\alpha=0.32}$	33.3870	0.7140	0.5885	**98.4375**	32.9632	0.6979	0.5802	**98.4375**
OSTB*	34.1781	0.7444	0.4303	**98.4375**	33.7417	0.7268	0.4328	**98.4375**

A.7. Additional Experiment: Ablation studies

Figures 4 and 5 show the ablation results in cross-altitude prediction scenarios where the output modality (h_{out}) is closer to the ground and the input modality (h_{in}) is much higher above from the ground.

A.8. Hyperparameter Search: Number of Residual Blocks in OSTB Model

We varied the number of residual blocks in our OSTB model and evaluated the different variants of the OSTB models with varying number of residual blocks on the validation dataset. The validation dataset consists of 200 data points. As we split each data sample into 4 sub-samples, the total number of effective validation data points becomes 800. Figures 6 and 7 show the results of the OSTB models with varying number of residual blocks. Figure 6 presents those cross-altitude prediction scenarios where the input modality h_{in} is closer to the ground and the output modality h_{out} is much higher above from the ground, and Figure 7 presents alternative cross-altitude prediction scenarios.

Figure 6 shows that OSTB model with 4 residual blocks consistently outperforms other variants of OSTB model across all three metrics. For the LPIPS metric, the differences among different variants of the OSTB model is almost indistinguishable.

Figure 7 shows similar trend of OSTB model with 4 residual blocks outperforming other variants of OSTB model across all three metrics in majority of the evaluation scenarios. For the LPIPS metric, the differences among different variants of the OSTB model is almost indistinguishable.

We observe that OSTB model with 4 residual blocks show more consistent performance than other variants of the OSTB models. Some variants with higher number of residual blocks show superior performance in some evaluation scenarios, but that will also increase the overall inference time. As a result, we chose the variant with 4 residual blocks as the main model throughout all the experiments conducted.

A.9. List of Notations

$\mathbf{x}_k^H$	Discrete high resolution data representation of modality k
$\mathcal{M}_k^H$	Discrete high resolution data space of modality k
$\mathbf{x}_k^L$	Discrete low resolution data representation of modality k
$\mathcal{M}_k^L$	Discrete low resolution data space of modality k
$\mathbf{X}_c$	Two-dimensional coordinate space
$\mathbf{x}^{(c)}$	Two-dimensional coordinate point
$\mathcal{M}_l^C(x^{(c)})$	Data space of target value at coordinate point $x^{(c)}$ for modality l

A.10. List of Abbreviations

OSTB	One-Stone Three Bird
INN	Implicit Neural Network
GAAM	Gaussian Adaptive Attention Mechanism
KAN	Kolmogorov-Arnold Network
LIIF	Local Implicit Image Function
INR	Implicit Neural Representation
MLP	Multi-Layer Perceptron
PSNR	Peak-Signal to Noise Ratio
SSIM	Structural Similarity Index Measure
LPIPS	Learned Perceptual Image Patch Similarity
CR	Compression Ratio
MAINN	Multi-Altitude Implicit Neural Network
GINO	Geometry-Informed Neural Operator
PPM	Prediction by Partial Matching

References

Hu J, Shen L and Sun G (2018) Squeeze-and-excitation networks. In *Proceedings of the IEEE conference on computer vision and pattern recognition*, 7132–7141.

Krizhevsky A, Sutskever I and Hinton GE (2012) ImageNet Classification with Deep Convolutional Neural Networks. In Pereira F, Burges C, Bottou L and Weinberger K (eds), *Advances in Neural Information Processing Systems*. vol 25. Curran Associates, Inc. Available at https://proceedings.neurips.cc/paper_files/paper/2012/file/c399862d3b9d6b76c8436e924a68c45b-Paper.pdf.

Simonyan K and Zisserman A (2014) Very deep convolutional networks for large-scale image recognition. *arXiv preprint arXiv:1409.1556*.

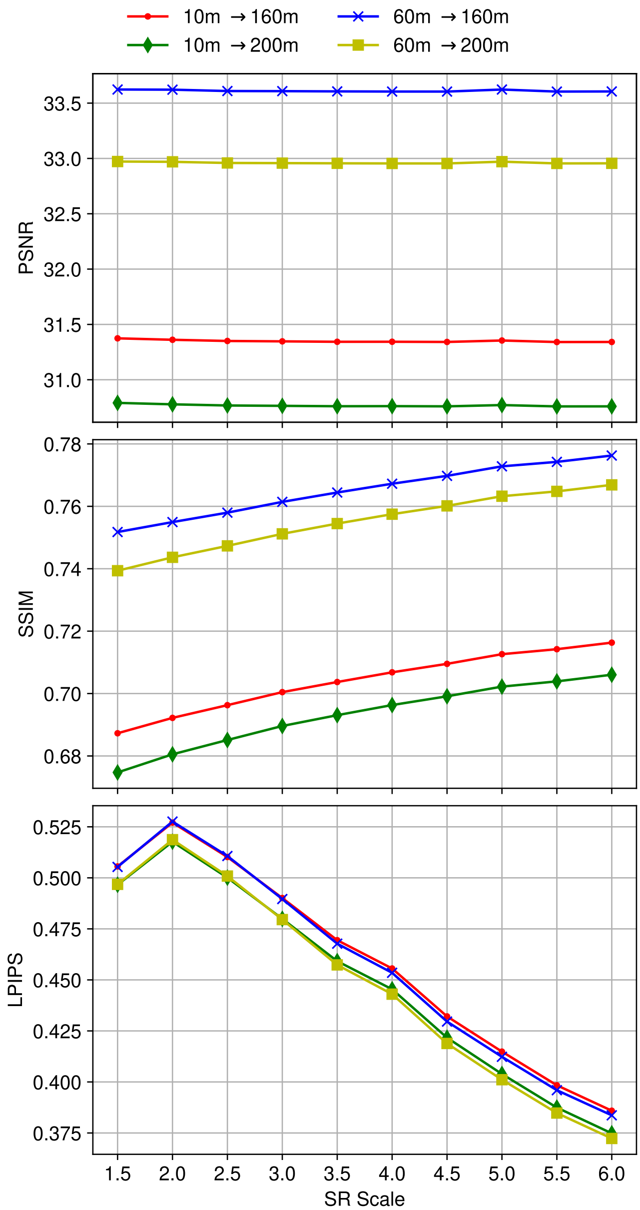

Figure 1. *Comparative Results of the OSTB model for differnet cross-altitude prediction scenarios. x−axis shows different super resolution scales for all three subplots, and y−axis shows the metric values (PSNR, SSIM and LPIPS metric values are shown in the three rows from top to bottom row accordingly).*

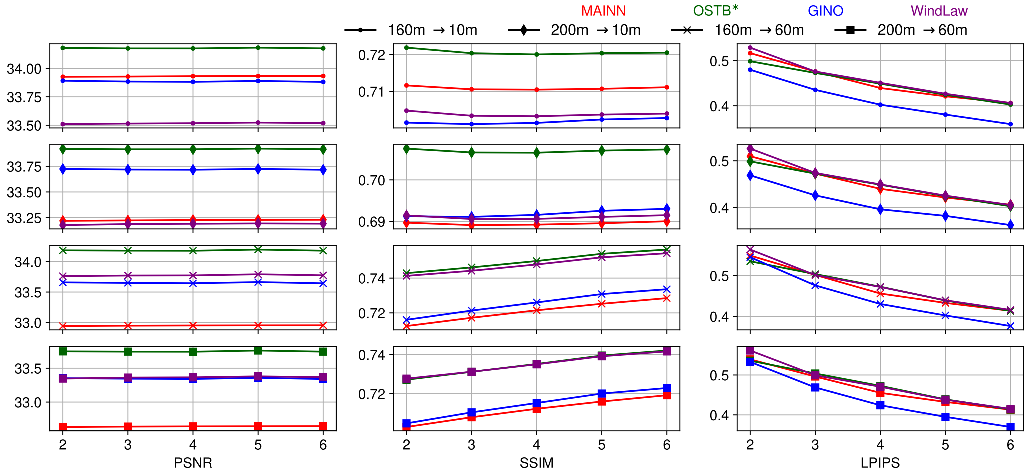

Figure 2. *Comparative Results with Baselines. x−axis shows different super resolution scales for all three subplots, and y−axis shows the metric values (PSNR, SSIM and LPIPS metric values are shown in the three columns from left to right column accordingly). The 4 rows show the evaluation results in 4 different cross-altitude prediction scenarios: $160m \longrightarrow 10m$, $200m \longrightarrow 10m$, $160m \longrightarrow 60m$ and $200m \longrightarrow 60m$ from top to bottom row accordingly.*

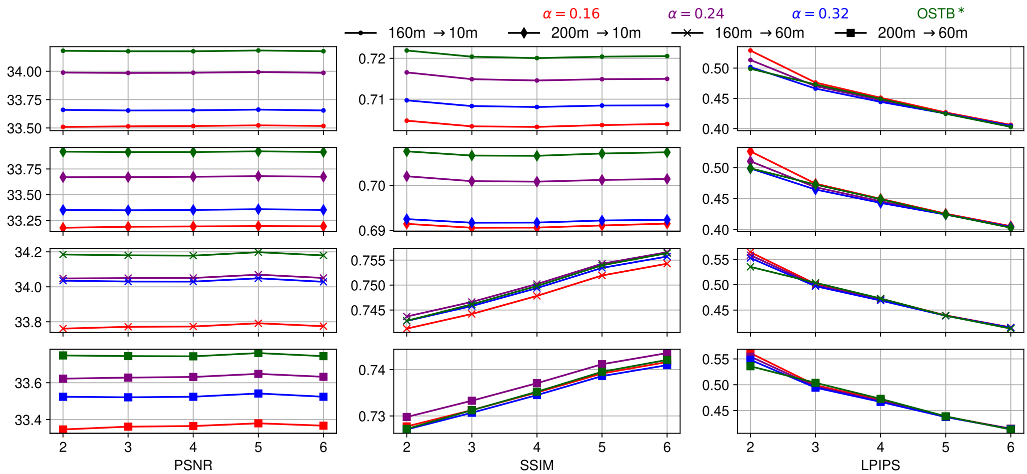

Figure 3. *Results for Modality Transfer Experiment. x−axis shows different super resolution scales for all three subplots, and y−axis shows the metric values (PSNR, SSIM and LPIPS metric values are shown in the three columns from left to right column accordingly). The 4 rows show the evaluation results in 4 different cross-altitude prediction scenarios: $160m \longrightarrow 10m$, $200m \longrightarrow 10m$, $160m \longrightarrow 60m$ and $200m \longrightarrow 60m$ from top to bottom row accordingly.*

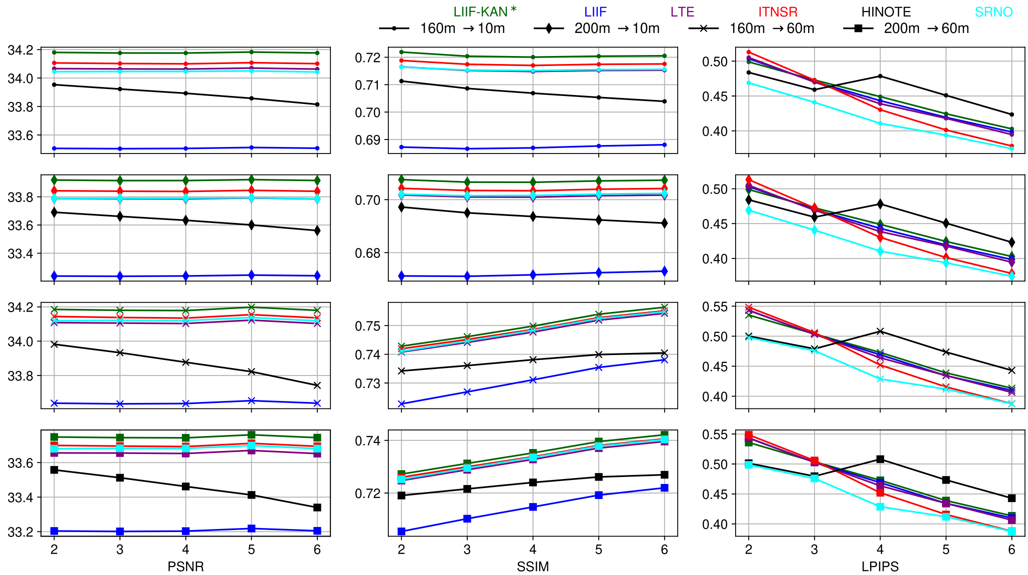

Figure 4. *Ablation of decoders. x−axis shows different super resolution scales for all three subplots, and y−axis shows the metric values (PSNR, SSIM and LPIPS metric values are shown in the three columns from left to right column accordingly). The 4 rows show the evaluation results in 4 different cross-altitude prediction scenarios:* $160m \rightarrow 10m$, $200m \rightarrow 10m$, $160m \rightarrow 60m$ *and* $200m \rightarrow 60m$ *from top to bottom row accordingly.*

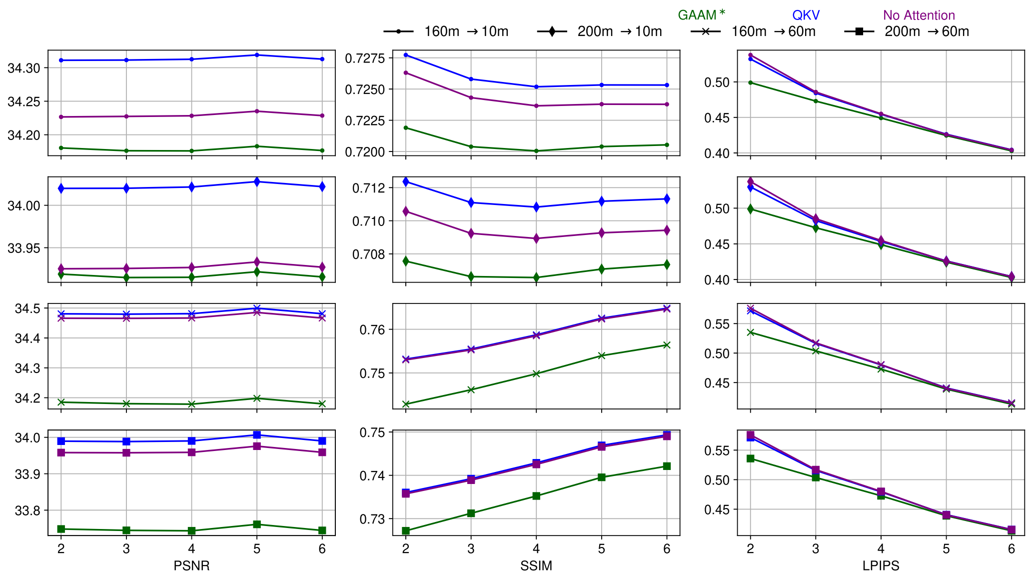

Figure 5. *Ablation of attention mechanism. x−axis shows different super resolution scales for all three subplots, and y−axis shows the metric values (PSNR, SSIM and LPIPS metric values are shown in the three columns from left to right column accordingly). The 4 rows show the evaluation results in 4 different cross-altitude prediction scenarios:* $160m \rightarrow 10m$, $200m \rightarrow 10m$, $160m \rightarrow 60m$ *and* $200m \rightarrow 60m$ *from top to bottom row accordingly.*

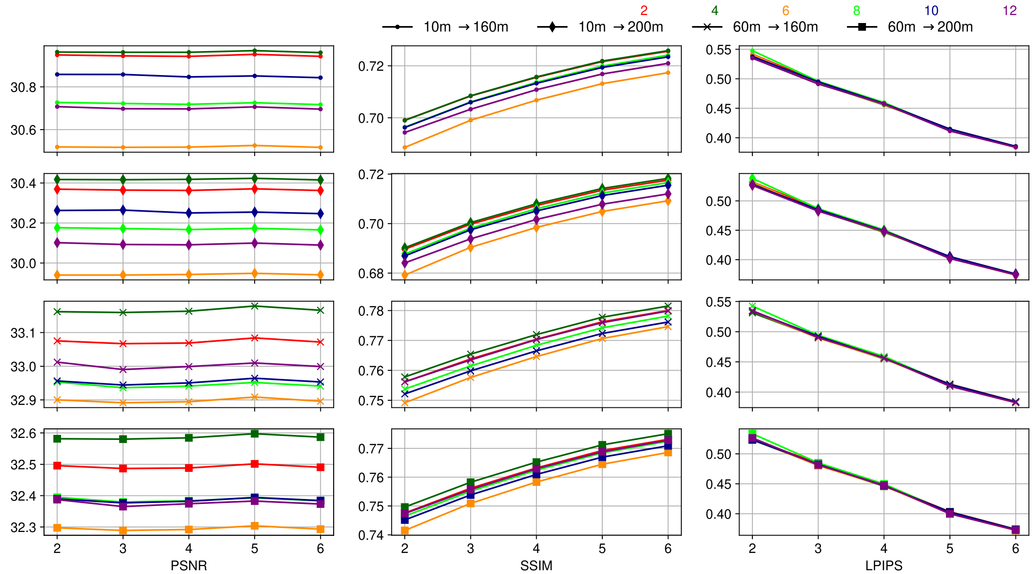

Figure 6. *Experimental results on the validation dataset of OSTB model with different number of residual blocks (cross-altitude prediction scenarios with $h_{in} < h_{low}$). $x-$axis shows different super resolution scales for all three subplots, and $y-$axis shows the metric values (PSNR, SSIM and LPIPS metric values are shown in the three columns from left to right column accordingly). The 4 rows show the evaluation results in 4 different cross-altitude prediction scenarios: $10m \rightarrow 160m$, $10m \rightarrow 200m$, $60m \rightarrow 160m$ and $60m \rightarrow 200m$ from top to bottom row accordingly.*

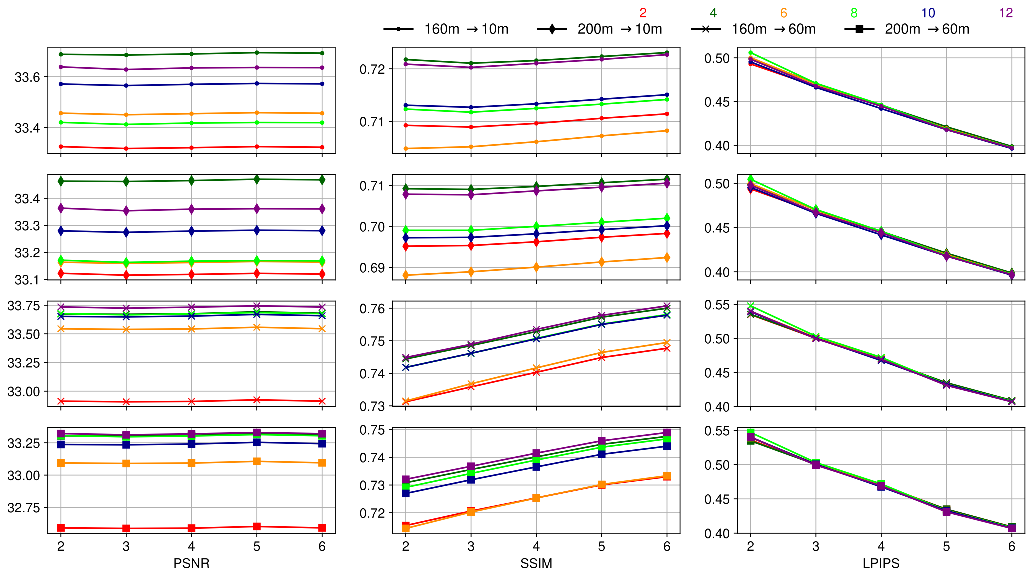

Figure 7. *Experimental results on the validation dataset of OSTB model with different number of residual blocks (cross-altitude prediction scenarios with $h_{in} > h_{low}$). $x-$axis shows different super resolution scales for all three subplots, and $y-$axis shows the metric values (PSNR, SSIM and LPIPS metric values are shown in the three columns from left to right column accordingly). The 4 rows show the evaluation results in 4 different cross-altitude prediction scenarios: $160m \rightarrow 10m$, $200m \rightarrow 10m$, $160m \rightarrow 60m$ and $200m \rightarrow 60m$ from top to bottom row accordingly.*